THE JOURNAL OF BIOLOGICAL CHEMISTRY VOL. 286, NO. 14, pp. 12086–12092, April 8, 2011

The CC′ and DE Loops in Ig Domains 1 and 2 of MAdCAM-1 Play Different Roles in MAdCAM-1 Binding to Low- and High-affinity Integrin $\alpha_4\beta_7$*[S]

Received for publication, December 3, 2010, and in revised form, January 19, 2011 Published, JBC Papers in Press, February 4, 2011, DOI 10.1074/jbc.M110.208900

Hao Sun[‡], YuMei Wu[‡], JunPeng Qi[‡], YouDong Pan[‡], Gaoxiang Ge[§], and JianFeng Chen[‡1]

From the [‡]Laboratory of Molecular Cell Biology and [§]State Key Laboratory of Molecular Biology, Institute of Biochemistry and Cell Biology, Shanghai Institutes for Biological Sciences, Chinese Academy of Sciences, Shanghai 200031, China

Lymphocyte homing is regulated by the dynamic interaction between integrins and their ligands. Integrin $\alpha_4\beta_7$ mediates both rolling and firm adhesion of lymphocytes by modulating its affinity to the ligand, mucosal addressin cell adhesion molecule-1 (MAdCAM-1). Although previous studies have revealed some mechanisms of $\alpha_4\beta_7$-MAdCAM-1 binding, little is known about the different molecular bases of the low- and high-affinity $\alpha_4\beta_7$-MAdCAM-1 interactions, which mediate rolling and firm adhesion of lymphocytes, respectively. Here, we found that two loops in immunoglobulin domains 1 and 2 (D1 and D2) of MAdCAM-1 played different roles in MAdCAM-1 binding to low-affinity (inactive) and high-affinity (activated) $\alpha_4\beta_7$. The Asp-42 in the CC′ loop of D1 was indispensable for MAdCAM-1 binding to both low-affinity and high-affinity $\alpha_4\beta_7$. The other CC′ loop residues except for Arg-39 and Ser-44 were essential for MAdCAM-1 binding to both inactive $\alpha_4\beta_7$ and $\alpha_4\beta_7$ activated by SDF-1α or talin, but not required for MAdCAM-1 binding to Mn^{2+}-activated $\alpha_4\beta_7$. Single amino acid substitution of the DE loop residues mildly decreased MAdCAM-1 binding to both inactive and activated $\alpha_4\beta_7$. Notably, removal of the DE loop greatly impaired MAdCAM-1 binding to inactive and SDF-1α- or talin-activated $\alpha_4\beta_7$, but only decreased 60% of MAdCAM-1 binding to Mn^{2+}-activated $\alpha_4\beta_7$. Moreover, DE loop residues were important for stabilizing the low-affinity $\alpha_4\beta_7$-MAdCAM-1 interaction. Thus, our findings demonstrate the distinct roles of the CC′ and DE loops in the recognition of MAdCAM-1 by low- and high-affinity $\alpha_4\beta_7$ and suggest that the inactive $\alpha_4\beta_7$ and $\alpha_4\beta_7$ activated by different stimuli have distinct conformations with different structural requirements for MAdCAM-1 binding.

Lymphocyte homing from circulation to lymphoid tissues and sites of inflammation is regulated by the dynamic interaction between lymphocyte integrin receptors and endothelial immunoglobulin superfamily cell adhesion molecules (1–3). Integrin $\alpha_4\beta_7$ is an important lymphocyte homing receptor that can mediate both rolling and firm adhesion of lymphocytes, two of the critical steps in lymphocyte migration and tissue-specific homing (4). Its ligand, MAdCAM-1,[2] is preferentially expressed on high endothelial venules of gut-associated lymphoid organs and on lamina propria venules, helping lymphocyte traffic to mucosal organs (5). The interaction between MAdCAM-1 and integrin $\alpha_4\beta_7$ is the key step in lymphocyte homing to gut and plays vital roles in both gut mucosal immune homeostasis and intestinal inflammation (6, 7).

Human MAdCAM-1 is a multidomain molecule consisting of two Ig-like domains followed by mucin-like sequences (8). Domain swapping experiments with MAdCAM-1 and VCAM-1 have demonstrated the requirement of the two Ig domains of MAdCAM-1 for efficient integrin $\alpha_4\beta_7$ binding (9). The crystal structure of MAdCAM-1 highlights two protruding loops from the two Ig domains, the CC′ loop in D1 and DE loop in D2, which are important for the interaction between MAdCAM-1 and $\alpha_4\beta_7$ (10, 11). The essential integrin-binding motif (LDTS) resides in the CC′ loop of MAdCAM-1 D1, and the Asp-42 in the LDTS motif serves as the primary $\alpha_4\beta_7$-binding site by directly interacting with the metal ion at the metal ion-dependent adhesion site (MIDAS) in the integrin β_7 I domain (8, 12–14). Mutational studies suggest that some other residues in the CC′ loop of MAdCAM-1 are also involved in MAdCAM-1-$\alpha_4\beta_7$ binding (9, 12, 13). The DE loop in D2 is predominated by negatively charged residues, which have been reported to play an important role in determining integrin binding specificity (15). Mutagenesis study has shown that some residues in the DE loop are important for MAdCAM-1 binding to integrin $\alpha_4\beta_7$ (9).

Integrins are α/β heterodimeric cell adhesion molecules that mediate cell-cell, cell-extracellular matrix, and cell-pathogen interactions and transmit signals bidirectionally across the plasma membrane (16–18). Cell adhesion through integrin is dependent on the dynamic regulation of integrin affinity. The low-affinity integrin $\alpha_4\beta_7$ mediates rolling adhesion of lymphocytes. Upon activation, $\alpha_4\beta_7$ converts to a high-affinity state, which mediates firm cell adhesion. Early studies on integrin structure have revealed that integrin extracellular domains exist in at least three distinct global conformational states: bent

* This work was supported by grants from the National Basic Research Program of China (Grant 2010CB529703), National Natural Science Foundation of China (Grants 30700119 and 30970604), the Chinese Academy of Sciences (Grant KSCX2-YW-R-67), and the Shanghai Pujiang Program (Grant 08PJ14106).

[S] The on-line version of this article (available at http://www.jbc.org) contains supplemental Fig. S1 and supplemental Videos S1–S5.

[1] To whom correspondence should be addressed: Institute of Biochemistry and Cell Biology, 320 YueYang Rd., Shanghai 200031, China. Tel.: 86-21-54921142; Fax: 86-21-54921658; E-mail: jfchen@sibs.ac.cn.

[2] The abbreviations used are: MAdCAM-1, mucosal cell adhesion molecule-1; MIDAS, metal ion-dependent adhesion site; ADMIDAS, adjacent to MIDAS; PBL, peripheral blood lymphocyte; hu, human.

with a closed headpiece, extended with a closed headpiece, and extended with an open headpiece, which correspond to the low-affinity, intermediate-affinity, and high-affinity states, respectively (19–21). The equilibrium among these different affinity states is regulated by integrin inside-out signaling and certain extracellular stimuli, such as divalent cations (22, 23). When compared with the low-affinity state in Ca^{2+} + Mg^{2+}, removal of Ca^{2+} or the addition of Mn^{2+} strikingly increases ligand binding affinity and adhesiveness of almost all integrins (14, 24–26). Crystal structures of $\alpha_V\beta_3$ and $\alpha_{IIb}\beta_3$ integrins revealed three interlinked metal ion-binding sites in integrin β I domain (27, 28). The central MIDAS is flanked by two metal ion-binding sites, the adjacent to MIDAS (ADMIDAS) site and the synergistic metal ion-binding site. The divalent cation at MIDAS directly coordinates the acidic side chain shared by all integrin ligands and is essential for integrin-ligand binding (14, 29). The synergistic metal ion-binding site and ADMIDAS function as positive and negative regulatory sites, respectively (14, 25, 30–32). Upon activation, integrin with the bent conformation converts to the extended conformation coupled with a series of global and local conformational changes, including separation of cytoplasmic tails, extension of integrin ectodomains, swing-out of the hybrid domain, β I domain α7 helix downward movement, and conformational rearrangement at the integrin ligand-binding site around MIDAS and ADMIDAS.

Despite the above advances in understanding of $\alpha_4\beta_7$-binding hotspots on MAdCAM-1 and integrin conformational rearrangement during activation, the molecular basis for the recognition of MAdCAM-1 by low- and high-affinity $\alpha_4\beta_7$ remains elusive. The mechanism of rolling and firm adhesion of lymphocyte mediated by $\alpha_4\beta_7$ on MAdCAM-1 is not well understood.

In this study, we found that the CC′ loop in D1 and DE loop in D2 of MAdCAM-1 exerted different functions in MAdCAM-1 binding to low- and high-affinity $\alpha_4\beta_7$. In addition, we demonstrated that the inactive $\alpha_4\beta_7$ and $\alpha_4\beta_7$ activated by different stimuli might have distinct conformations with different structural requirements for MAdCAM-1 binding.

EXPERIMENTAL PROCEDURES

Cells and Reagents—cDNAs of human α_4 and β_7 were constructed in vector pcDNA3.1/Hygro(−) (Invitrogen). cDNA of mouse talin head domain (talin 1–435) with N-terminal-fused GFP (GFP-talin-head) in vector pcDNA3.1 was kindly provided by Dr. Minsoo Kim. All constructs were confirmed by DNA sequencing. Transient transfection of 293T cells was performed as described (14). 293T cells stably expressing integrin $\alpha_4\beta_7$ were established by co-transfection of human α_4/β_7 cDNAs and selected by hygromycin (0.2 mg/ml). The expression level of integrin $\alpha_4\beta_7$ was determined by immunofluorescence flow cytometry. Act-1 mAb specific for integrin $\alpha_4\beta_7$ was as described previously (33). Recombinant human SDF-1α was from R&D Systems Inc.

Isolation of Peripheral Blood Lymphocytes (PBLs)—Peripheral venous blood from normal donors was collected using anticoagulant citrate dextrose as an anticoagulant. Human peripheral blood mononuclear cells were isolated from buffy coats using a Ficoll density gradient, washed, and suspended in RPMI 1640 (Invitrogen), supplemented with 100 μg/ml penicillin, 100 μg/ml streptomycin, 2 mM glutamine (all from Invitrogen), and 10% (v/v) FBS (Biocherom AG, Germany). Monocytes were depleted by incubation on tissue culture plastic for 30 min at 37 °C. The lymphocytes were rich in the supernatant fluid.

HuMAdCAM-1-Fc Cloning and Expression—Human MAdCAM-1 (from Val-1 to Pro-315) fused to the Fc1 and Fc2 regions of human IgG1 (huMAdCAM-1/Fc) was constructed in vector pcDNA3.0 (Invitrogen). Site-directed mutations were introduced into MAdCAM-1 cDNA using QuikChange (Stratagene). 293T cells were transiently transfected with huMAdCAM-1/Fc construct and cultured for 3–4 days in a humidified atmosphere of 5% (v/v) CO_2 at 37 °C. The huMAdCAM-1/Fc was isolated from conditioned medium by protein A-Sepharose (Pierce) and further purified by gel filtration in 20 mM HEPES, 300 mM NaCl, pH 7.4 (HEPES-buffered saline).

Flow Chamber Assay—The flow chamber assay was performed as described (25). A polystyrene Petri dish was coated with a 5-mm diameter, 20-μl spot of 10 μg/ml purified huMAdCAM-1/Fc in coating buffer (PBS, 10 mM $NaHCO_3$, pH 9.0) for 1 h at 37 °C followed by 2% BSA in coating buffer for 1 h at 37 °C to block nonspecific binding sites. Cells were washed twice with Ca^{2+}- + Mg^{2+}-free HEPES-buffered saline (20 mM Hepes, pH 7.4, 5 mM EDTA, 0.5% BSA), resuspended at 1×10^7/ml in buffer A (Ca^{2+}- + Mg^{2+}-free HEPES-buffered saline, 0.5% BSA), and kept at room temperature. Cells were diluted to 1×10^6/ml in buffer A containing different divalent cations immediately before infusion in the flow chamber using a Harvard apparatus programmable syringe pump. Cells were allowed to accumulate for 30 s at 0.3 dyne/cm^2 and 10 s at 0.4 dyne/cm^2. Then, shear stress was increased every 10 s from 1 dyne/cm^2 up to 16 dynes/cm^2 in 2-fold increments. The number of cells remaining bound at the end of each 10-s interval was determined. Rolling velocity at each shear stress was calculated from the average distance traveled by rolling cells in 3 s. To avoid confusing rolling with small amounts of movement due to tether stretching or measurement error, a velocity of 2 μm/s, which corresponds to a movement of one-half cell diameter during the 3-s measurement interval, was the minimum velocity required to define a cell as rolling instead of firmly adherent.

SDF-1α Stimulation Assay under Flow—A polystyrene Petri dish was coated with a 5-mm diameter, 20-μl spot of 10 μg/ml purified huMAdCAM-1/Fc with SDF-1α (2 μg/ml) or huMAdCAM-1/Fc alone in coating buffer for 1 h at 37 °C followed by 2% BSA in coating buffer for 1 h at 37 °C to block nonspecific binding sites. The PBLs (1×10^6/ml) were infused into the chamber, and then cells were allowed to settle for 2 min and to accumulate for 30 s at 0.3 dyne/cm^2 and 10 s at 0.4 dyne/cm^2. Then, shear stress was increased every 10 s from 1 dyne/cm^2 up to 16 dynes/cm^2, in 2-fold increments. Cells remaining bound under the wall shear stress of 1 dyne/cm^2 were counted. The PBLs (1×10^6/ml) preincubated with $\alpha_4\beta_7$-blocking mAb Act-1 (2 μg/ml) or treated with 5 mM EDTA were used as control.

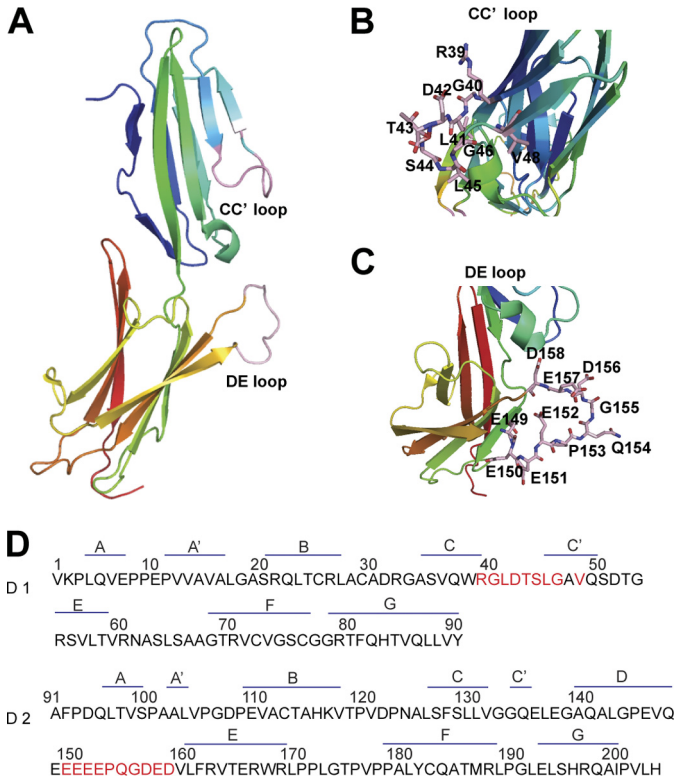

FIGURE 1. **Structure and sequence of human MAdCAM-1 D1/D2.** *A*, the N-terminal two-domain fragment of human MAdCAM-1 (Protein Data Bank (PDB) 1gsm) (11). The CC′ and DE loops reside in D1 and D2, respectively. *B* and *C*, the detailed view of the CC′ and DE loops. The amino acid residues in the CC′ and in the DE loops were shown in *B* and *C*, respectively. *D*, amino acid sequences of human MAdCAM-1 D1 and D2. The residues chosen for single amino acid substitution by Ala are highlighted in *red*.

RESULTS

To study the molecular basis for the recognition of MAdCAM-1 by low- and high-affinity integrin $\alpha_4\beta_7$, we generated soluble human MAdCAM-1 protein (from Val-1 to Pro-315), which contains domain 1, domain 2, and mucin-like domain with C-terminal fused Fc1 and two regions of human IgG1. Because the CC′ loop in D1 of MAdCAM-1 possesses the LDTS motif, which has been implicated as the primary integrin-binding site, we first investigated the function of the CC′ loop in the binding of low- and high-affinity integrin $\alpha_4\beta_7$ to MAdCAM-1 by introducing a series of single point mutations in the CC′ loop based on the MAdCAM-1 crystal structure (Fig. 1) (10, 11).

Asp-42 in CC′ Loop of MAdCAM-1 D1 Is Essential for MAdCAM-1 Binding to Both Low-affinity and High-affinity $\alpha_4\beta_7$—Adhesive behavior of 293T cells stably expressing human integrin $\alpha_4\beta_7$ in shear flow was characterized in a parallel wall flow chamber by allowing them to adhere to MAdCAM-1 adsorbed to the lower wall. The shear stress was incrementally increased, and the velocity of the cells remaining bound at each increment was determined. Human $\alpha_4\beta_7$ 293T transfectants behaved as described previously for lymphoid cells expressing $\alpha_4\beta_7$ (26). In 1 mM Ca^{2+} + 1 mM Mg^{2+}, about 90% of the bound $\alpha_4\beta_7$ transfectants rolled at the shear stress of 1 dyne/cm^2 (Fig. 2*A*). By contrast, cells were firmly adherent in 0.5 mM Mn^{2+} (Fig. 2*B*). Rolling and firm adhesion represent the low- and high-affinity interactions of $\alpha_4\beta_7$ with MAdCAM-1,

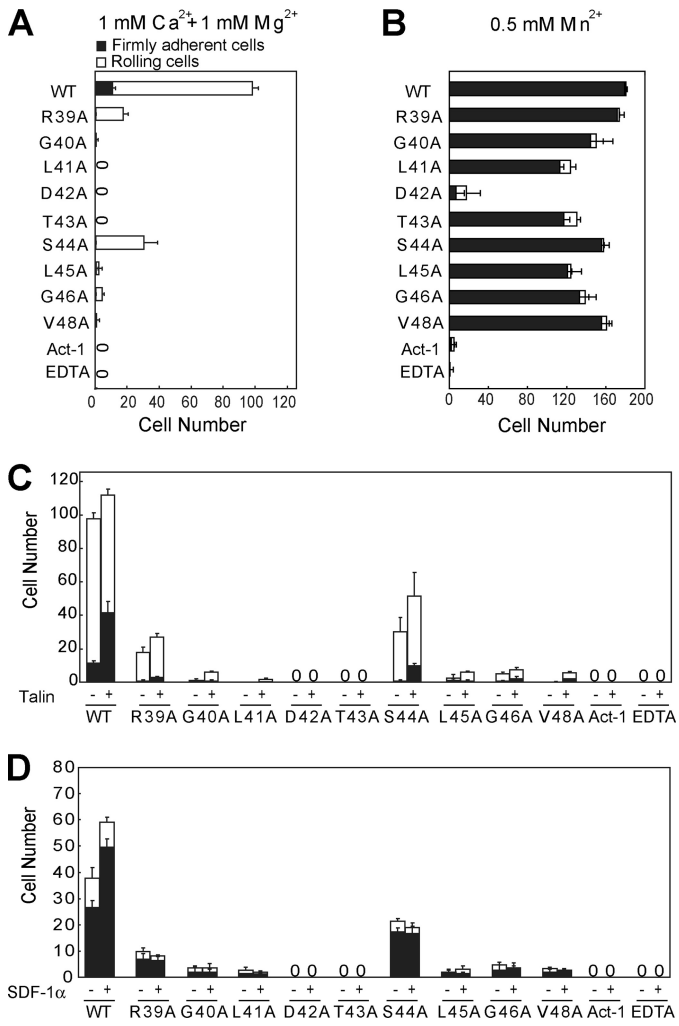

FIGURE 2. **Effect of the CC′ loop point mutations on $\alpha_4\beta_7$-mediated cell adhesion on MAdCAM-1 substrates in shear flow.** *A–C*, rolling and firm adhesion on MAdCAM-1 substrates of $\alpha_4\beta_7$ 293T stable transfectants in 1 mM Ca^{2+} + 1 mM Mg^{2+} (*A*), in 0.5 mM Mn^{2+} (*B*), or before and after transfection with GFP-talin-head in 1 mM Ca^{2+} + 1 mM Mg^{2+} (*C*). *D*, adhesive modality of human PBLs on MAdCAM-1 substrates in 1 mM Ca^{2+} + 1 mM Mg^{2+} before and after stimulation with SDF-1α. The number of rolling and firmly adherent cells was measured in the indicated divalent cations at a wall shear stress of 1 dyne/cm^2. The experiment was performed on the surface coated with WT or mutant MAdCAM-1 (10 μg/ml). The cells preincubated with the $\alpha_4\beta_7$ blocking mAb Act-1 (2 μg/ml) at 37 °C for 5 min or treated with 5 mM EDTA were used as control. *Error bars* are ±S.D. (n = 3). Representative videos are shown as supplemental Videos S1–S5.

respectively. As control, $\alpha_4\beta_7$transfectants treated with $\alpha_4\beta_7$ blocking antibody Act-1 or with 5 mM EDTA did not accumulate on MAdCAM-1 substrates (Fig. 2, *A* and *B*). In contrast to the robust cell adhesion on WT MAdCAM-1, substitution of Asp-42 with Ala abolished both rolling and firm adhesion on MAdCAM-1 mediated by the low-affinity $\alpha_4\beta_7$ in 1 mM Ca^{2+} + 1 mM Mg^{2+} and high-affinity $\alpha_4\beta_7$ in 0.5 mM Mn^{2+}, suggesting its essential role in integrin-ligand binding (Fig. 2, *A* and *B*).

In Addition to Asp-42, other CC′ Loop Residues Except for Arg-39 and Ser-44 Are Essential for MAdCAM-1 Binding to Low-affinity $\alpha_4\beta_7$—When compared with the efficient rolling cell adhesion on WT MAdCAM-1, single amino acid substitution of most residues in the MAdCAM-1 CC′ loop with Ala abolished the rolling cell adhesion on MAdCAM-1 mediated by low-affinity $\alpha_4\beta_7$ in 1 mM Ca^{2+} + 1 mM Mg^{2+} (Fig. 2*A*). Arg-39

and Ser-44 to Ala mutations showed less effect, which led to 70 and 80% decrease of cell adhesion to MAdCAM-1, respectively.

CC′ Loop Residues Other than Asp-42 Are Not Important for MAdCAM-1 Binding to High-affinity $\alpha_4\beta_7$ Activated by Mn^{2+}—In contrast to rolling cell adhesion mediated by low-affinity $\alpha_4\beta_7$, the firm cell adhesion mediated by Mn^{2+}-activated $\alpha_4\beta_7$ was only slightly affected by the same mutations, except for Asp-42 (Fig. 2*B*). More than 70% of cell adhesion was retained when Leu-41, Thr-43, Leu-45, and Gly-46 were mutated to Ala, respectively. The rest of the mutations only caused less than 10% loss of cell adhesion in Mn^{2+}. Thus, except for the primary MAdCAM-1-$\alpha_4\beta_7$-binding site Asp-42, the rest of the CC′ residues other than Arg-39 and Ser-44 in the CC′ loop are essential for the interaction between low-affinity $\alpha_4\beta_7$ and MAdCAM-1, but not required for the binding of Mn^{2+}-activated $\alpha_4\beta_7$ to MAdCAM-1.

CC′ Loop Residues Other than Arg-39 and Ser-44 Are Crucial for MAdCAM-1 Interaction with High-affinity Integrin $\alpha_4\beta_7$ Activated by Talin or SDF-1α—Besides the unphysiological strong activation by Mn^{2+}, integrin can be activated by more physiological pathways such as overexpression of intracellular talin or SDF-1α stimulation (34). Talin is a cytoskeletal protein that can interact with the cytoplasmic tail of the integrin β subunit and activate integrin. To investigate the influence of the CC′ loop mutations on the interaction between MAdCAM-1 and talin-activated $\alpha_4\beta_7$, we overexpressed the GFP-talin-head in $\alpha_4\beta_7$ 293T transfectants (supplemental Fig. S1) and examined the cell adhesion behavior to WT and mutant MAdCAM-1 under flow (Fig. 2*C*). The firmly adherent $\alpha_4\beta_7$ transfectants on WT MAdCAM-1 increased from 11 to 37% of total bound cells under the shear stress of 1 dyne/cm^2 after co-transfection with GFP-talin-head, suggesting the activation of integrin $\alpha_4\beta_7$ by talin. Surprisingly, unlike the mild effects of the CC′ mutations on the cell adhesion mediated by Mn^{2+}-activated $\alpha_4\beta_7$ to MAdCAM-1, the cell adhesion mediated by talin-activated $\alpha_4\beta_7$ was greatly disrupted by most CC′ loop mutations. GFP-talin-head overexpression only slightly increased cell adhesion on R39A, G40A, S44A, L45A, G46A, and V48A mutants. R39A and S44A showed less effect, which led to 76 and 54% decrease of cell adhesion mediated by talin-activated $\alpha_4\beta_7$ to MAdCAM-1. Thus, the above results suggest that the CC′ loop residues other than Arg-39 and Ser-44 are crucial for the recognition of MAdCAM-1 by talin-activated $\alpha_4\beta_7$ and that integrin $\alpha_4\beta_7$ activated by Mn^{2+} and talin could have different conformations with different structural requirements for MAdCAM-1 binding.

Because the CC′ loop might play different roles in MAdCAM-1 interaction with Mn^{2+}- and talin-activated $\alpha_4\beta_7$, we next tested its function in the interaction between MAdCAM-1 and $\alpha_4\beta_7$ activated by SDF-1α. SDF-1α can induce integrin activation through the PI3 kinase pathway by binding to CXCR4, the G protein-coupled receptor of SDF-1α (35, 36). Human PBLs were used that express high levels of integrin $\alpha_4\beta_7$ (37) and CXCR4 (38). In contrast to the robust cell adhesion to WT MAdCAM-1 in 1 mM Ca^{2+} + 1 mM Mg^{2+}, PBL adhered weakly to most CC′ loop mutants and did not adhere to D42A and T43A mutants at all (Fig. 2*D*). R39A and S44A mutations showed less effect, which led to 86 and 68% decrease of cell adhesion to MAdCAM-1, respectively. Activation of $\alpha_4\beta_7$ by SDF1-α stimulation notably increased the number of PBLs bound to WT MAdCAM-1, but not to the MAdCAM-1 CC′ loop mutants, suggesting the importance of the CC′ loop residues in the interaction between MAdCAM-1 and $\alpha_4\beta_7$ activated by SDF1-α (Fig. 2*D*). Interestingly, cell adhesion to the MAdCAM-1 CC′ loop mutants could be increased by talin but not SDF1-α, indicating the subtle difference between integrins activated by talin and SDF-1α (Fig. 2, *C* and *D*).

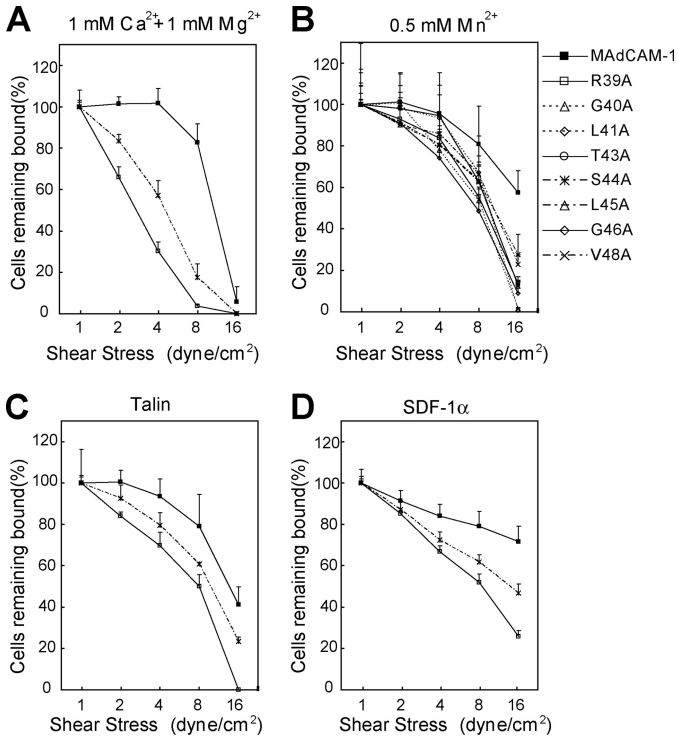

FIGURE 3. **Effect of the CC′ loop mutation on the strength of $\alpha_4\beta_7$-mediated adhesion to MAdCAM-1.** *A–C*, resistance to detachment of $\alpha_4\beta_7$ 293T transfectants at increasing wall shear stresses in 1 mM Ca^{2+} + 1 mM Mg^{2+} (*A*), in 0.5 mM Mn^{2+} (*B*), or in 1 mM Ca^{2+} + 1 mM Mg^{2+} after transfection with GFP-talin-head (*C*). *D*, resistance to detachment of human PBL stimulated with SDF-1α in 1 mM Ca^{2+} + 1 mM Mg^{2+}. The total number of cells remaining bound at each indicated wall shear stress was determined as a percentage of adherent cells at 1 dyne/cm^2. The experiment was performed on the surface coated with WT or mutant MAdCAM-1 (10 μg/ml). *Error bars* are ±S.D. ($n = 3$).

Taken together, the above data demonstrate that Asp-42 in the CC′ loop is essential for MAdCAM-1 binding to both low-affinity and high-affinity $\alpha_4\beta_7$, and the rest of the CC′ loop residues other than Arg-39 and Ser-44 are crucial for MAdCAM-1 binding to $\alpha_4\beta_7$ activated by physiological stimuli as SDF-1α or talin, but not required for MAdCAM-1 binding to $\alpha_4\beta_7$ activated by Mn^{2+}. Thus, integrins activated by distinct stimuli might have different high-affinity conformations with diverse structural requirements for MAdCAM-1 binding.

CC′ Loop Is Required for the Stable Interaction between MAdCAM-1 and Low-affinity Integrin $\alpha_4\beta_7$—To test the effect of the CC′ loop on the strength of $\alpha_4\beta_7$-mediated cell adhesion to MAdCAM-1, we examined the resistance of adherent cells to detachment by increasing shear stress (Fig. 3). MAdCAM-1 R39A and S44A mutants were chosen for studies on low-affinity $\alpha_4\beta_7$ in Ca^{2+} + Mg^{2+} and high-affinity $\alpha_4\beta_7$ activated by talin or SDF-1α because they were the only CC′ loop mutants

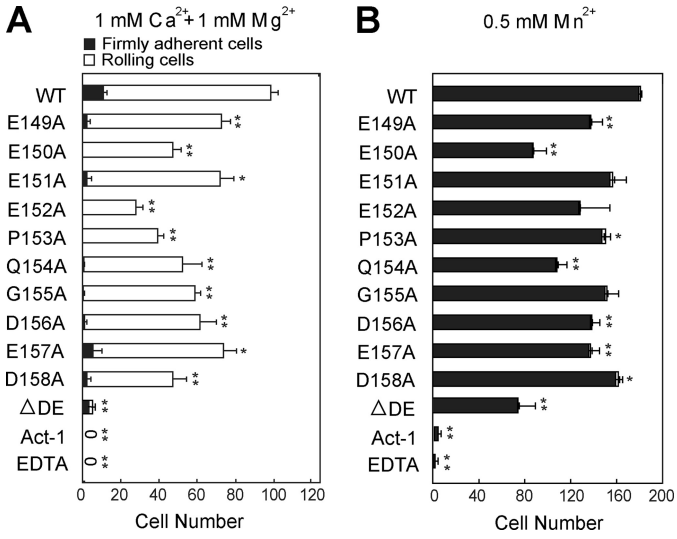

FIGURE 4. **Effect of the DE loop point mutations on $\alpha_4\beta_7$-mediated cell adhesion on MAdCAM-1 substrates in shear flow.** *A* and *B*, rolling and firm adhesion on MAdCAM-1 substrates of $\alpha_4\beta_7$ 293T transfectants in 1 mM Ca^{2+} + 1 mM Mg^{2+} (*A*) and 0.5 mM Mn^{2+} (*B*). The number of rolling and firmly adherent $\alpha_4\beta_7$ 293T transfectants was measured in the indicated divalent cations at a wall shear stress of 1 dyne/cm^2. The experiment was performed on the surface coated with WT or mutant MAdCAM-1 (10 μg/ml). The cells preincubated with the $\alpha_4\beta_7$ blocking mAb Act-1 (2 μg/ml) at 37 °C for 5 min or treated with 5 mM EDTA were used as control. *Error bars* are ±S.D. ($n = 3$). *, $p < 0.05$, **, $p < 0.01$, when compared with MAdCAM-1 WT.

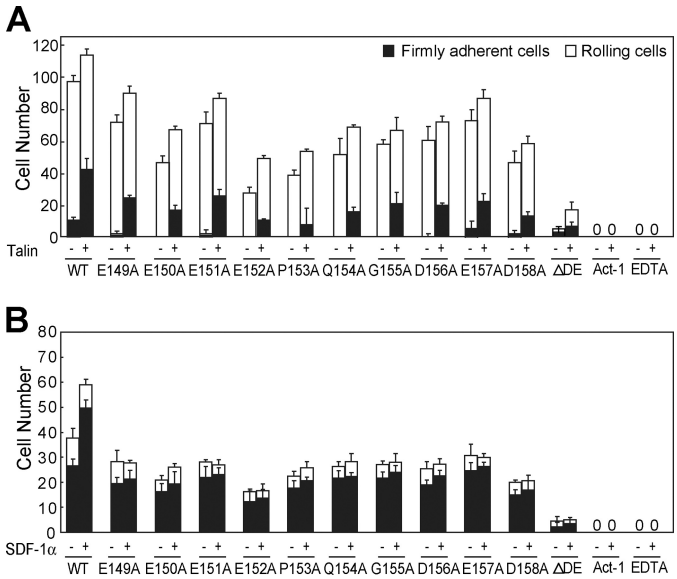

FIGURE 5. **Effect of DE loop mutations on MAdCAM-1 binding to integrin $\alpha_4\beta_7$ activated by talin or SDF-1α.** *A*, rolling and firm adhesion on MAdCAM-1 substrates of $\alpha_4\beta_7$ 293T transfectants before and after transfection with GFP-talin-head. *B*, rolling and firm adhesion on MAdCAM-1 substrates of human PBLs before and after stimulation with SDF-1α. The number of rolling and firmly adherent cells was measured at a wall shear stress of 1 dyne/cm^2. The experiment was performed on the surface coated with WT or mutant MAdCAM-1 (10 μg/ml). The cells preincubated with the $\alpha_4\beta_7$ blocking mAb Act-1 (2 μg/ml) at 37 °C for 5 min or treated with 5 mM EDTA were used as control. *Error bars* are ±S.D. ($n = 3$).

supporting clearly detectable cell adhesion under those conditions. In 1 mM Ca^{2+} + 1 mM Mg^{2+}, $\alpha_4\beta_7$ 293T transfectants detached more rapidly from the R39A and S44A mutants than from the WT MAdCAM-1 (Fig. 3*A*), suggesting the less stable interaction between integrin and the mutant ligands. In contrast, adhesion of cells bearing high-affinity $\alpha_4\beta_7$ activated by Mn^{2+}, talin, or SDF-1α to the MAdCAM-1 CC′ loop mutants was much less susceptible to the increased shear stress (Fig. 3, *B–D*).

The Intact DE Loop Is Essential for MAdCAM-1 Binding to Low-affinity $\alpha_4\beta_7$, but Not for Its Binding to High-affinity $\alpha_4\beta_7$ Activated by Mn^{2+}—To further define the different structural requirements for MAdCAM-1 binding to inactive and activated integrin $\alpha_4\beta_7$, we generated a series of single amino acid substitutions and a partial deletion (ΔDE, from Glu-152 to Asp-158) of the DE loop in MAdCAM-1 D2. MAdCAM-1 with deletion of the whole DE loop (from Glu-149 to Asp-158) could not be expressed. All of the single amino acid substitutions by Ala in the DE loop (residue 149–158) decreased the cell adhesion mediated by both low-affinity and high-affinity $\alpha_4\beta_7$ on MAdCAM-1, but to a different extent (Fig. 4*A*). For the rolling cell adhesion mediated by low-affinity $\alpha_4\beta_7$ on MAdCAM-1 in 1 mM Ca^{2+} + 1 mM Mg^{2+}, substitution of Glu-152 and Glu-153 by Ala led to an ~70 and 60% decrease of adherent cells, respectively. E150A, E154A, and D158A showed less effect, which resulted in an ~50% decrease (Fig. 4*A*). Other point mutations had even milder impact, retaining from 60 to 80% of adherent cells. For the firm cell adhesion mediated by high-affinity $\alpha_4\beta_7$ in Mn^{2+}, most DE loop point mutations showed much milder effects, except for Glu-150 and Glu-154, which led to 50 and 40% decrease of bound cells, respectively (Fig. 4*B*). Notably, the DE loop residues that mostly affected MAdCAM-1 interaction with low-affinity and high-affinity $\alpha_4\beta_7$ are different, suggesting the different roles of the DE loop residues in the recognition of integrin $\alpha_4\beta_7$ before and after activation. Different from single amino acid substitutions, the partial deletion of the DE loop abolished the interaction between low-affinity $\alpha_4\beta_7$ and MAdCAM-1, but only caused about 60% loss of cell adhesion to MAdCAM-1 mediated by the Mn^{2+}-activated $\alpha_4\beta_7$. The data demonstrate that the intact DE loop is essential to MAdCAM-1 binding to low-affinity $\alpha_4\beta_7$, but not to high-affinity $\alpha_4\beta_7$ activated by Mn^{2+}.

The Intact DE Loop Is Required for MAdCAM-1 Binding to Integrin $\alpha_4\beta_7$ Activated by Talin and SDF-1α—To further study the function of the DE loop in MACAM-1 binding to activated $\alpha_4\beta_7$, we examined the impact of DE loop deletion on the interaction between MAdCAM-1 and $\alpha_4\beta_7$ activated by talin and SDF-1α. Opposite to the partial rescued cell adhesion to ΔDE MAdCAM-1 after $\alpha_4\beta_7$ was activated by Mn^{2+}, the activation of $\alpha_4\beta_7$ by either talin or SDF-1α did not rescue the abolishment of cell adhesion by DE loop deletion in 1 mM Ca^{2+} + 1 mM Mg^{2+} (Fig. 5). Thus, the intact DE loop is important for MAdCAM-1 interaction with both low-affinity and high-affinity integrin $\alpha_4\beta_7$ activated by talin or SDF-1α. On the other hand, $\alpha_4\beta_7$ activated by Mn^{2+} could support decent cell adhesion to MAdCAM-1 in the absence of the intact DE loop, suggesting that the conformation of Mn^{2+}-activated $\alpha_4\beta_7$ may be different from those of the low-affinity and high-affinity $\alpha_4\beta_7$ activated by more physiological stimuli. The overexpression of GFP-talin-head augmented the firm adhesion of $\alpha_4\beta_7$ 293T transfectants on both WT and DE loop single residue mutant MAdCAM-1 (Fig. 5*A*). In contrast, SDF-1α stimulation increased the PBL adhesion only to the WT MAdCAM-1, but not to the DE loop mutants (Fig. 5*B*). These data suggest that the residues in the DE loop might be involved in distinguishing

the subtle difference between $\alpha_4\beta_7$ activated by talin and $\alpha_4\beta_7$ activated by SDF-1α.

The DE Loop Is Required for the Stable Interaction between MAdCAM-1 and Low-affinity Integrin $\alpha_4\beta_7$—Next, we investigated the function of the DE loop in the strength of $\alpha_4\beta_7$-mediated cell adhesion to MAdCAM-1 (Fig. 6). In 1 mM Ca^{2+} + 1 mM Mg^{2+}, the DE loop mutations significantly decreased the shear resistance of adherent cells bearing low-affinity $\alpha_4\beta_7$ (Fig. 6*A*). In contrast, the same mutations showed little effect on the stability of adhesion mediated by high-affinity $\alpha_4\beta_7$ activated by Mn^{2+}, talin, or SDF-1α (Fig. 6, *B–D*). Thus, the residues in the DE loop of MAdCAM-1 are important for stabilizing the interaction between low-affinity $\alpha_4\beta_7$ and MAdCAM-1.

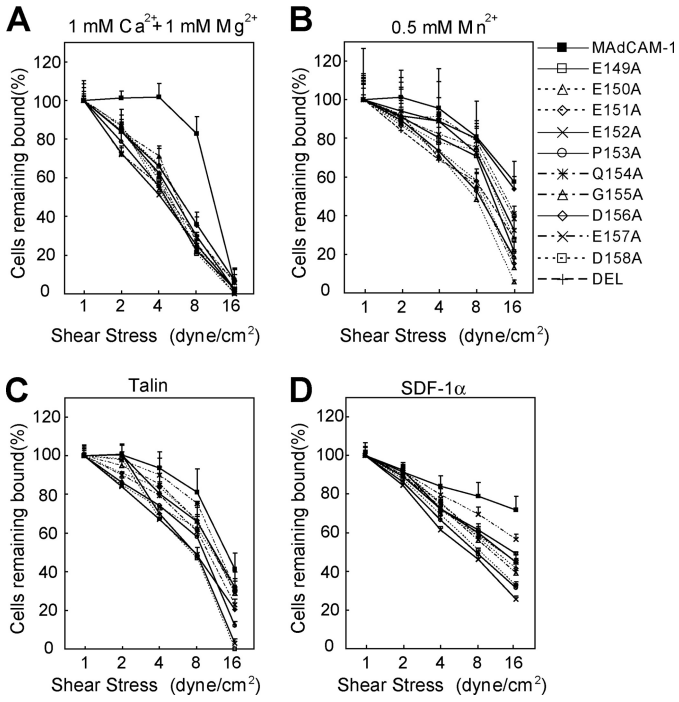

FIGURE 6. **Effect of the DE loop on the strength of $\alpha_4\beta_7$-mediated adhesion to MAdCAM-1.** *A–C*, resistance to detachment of $\alpha_4\beta_7$ 293T transfectants at increasing wall shear stresses in 1 mM Ca^{2+} + 1 mM Mg^{2+} (*A*), in 0.5 mM Mn^{2+} (*B*), or in 1 mM Ca^{2+} + 1 mM Mg^{2+} after transfection with GFP-talin-head (*C*). *D*, resistance to detachment of human PBL stimulated with SDF-1α. The total number of cells remaining rolling and firmly adherent at increasing wall shear stress was determined as a percentage of adherent cells at 1 dyne/cm^2. The experiment was performed on the surface coated with WT or mutant MAdCAM-1 (10 μg/ml). *Error bars* are ±S.D. (n = 3).

DISCUSSION

Lymphocyte homing to gut is dependent on the interaction between integrin $\alpha_4\beta_7$ and MAdCAM-1. The resting (low-affinity) and activated (high-affinity) integrin $\alpha_4\beta_7$ can mediate rolling and firm adhesion of lymphocytes, respectively, which are two of the critical steps in lymphocyte homing. Previous studies have shown that integrin undergoes global and local conformational changes upon activation, resulting in the distinct conformations of low-affinity and high-affinity integrins. Thus, it is tempting to speculate that the low-affinity and high-affinity $\alpha_4\beta_7$ binds MAdCAM-1 differently, which might play a fundamental role in supporting the rolling and firm cell adhesion. The integrin $\alpha_4\beta_7$-MAdCAM-1 interaction is dependent on a conserved acidic peptide motif in the first Ig-like domain of MAdCAM-1, which is present as a surface-exposed structure. The Asp-42 in this motif forms the primary interaction with the divalent cation at β_7 MIDAS. Because the primary interaction between Asp-42 and the MIDAS metal ion is shared by both low-affinity and high-affinity $\alpha_4\beta_7$-MAdCAM-1 binding, there should be other interactions between MAdCAM-1 and $\alpha_4\beta_7$ that determine rolling or firm adhesion.

Although previous studies have revealed that some residues in MAdCAM-1 are important for MAdCAM-1-$\alpha_4\beta_7$ binding (9, 12, 13, 15), the structural basis for supporting MAdCAM-1-$\alpha_4\beta_7$-mediated rolling and firm cell adhesion remains elusive because the static cell adhesion assay used in those studies is unable to distinguish rolling and firm cell adhesion. In this study, we used a flow chamber assay to screen the critical residues in MAdCAM-1, which are important for supporting rolling and firm cell adhesions, respectively. Our results demonstrate that the CC′ and DE loops play distinct roles in the recognition of MAdCAM-1 by low- and high-affinity $\alpha_4\beta_7$ and suggest that the inactive $\alpha_4\beta_7$ and $\alpha_4\beta_7$ activated by different stimuli have distinct conformations with different structural requirements for MAdCAM-1 binding (Fig. 7).

The Asp-42 in the CC′ loop is required for both low-affinity $\alpha_4\beta_7$-mediated rolling adhesion and high-affinity $\alpha_4\beta_7$-mediated firm adhesion. In addition to Asp-42, most other CC′ loop residues other than Arg-39 and Ser-44 are essential for the low-affinity $\alpha_4\beta_7$-MAdCAM-1 interaction, suggesting the potential binding sites at the CC′ loop for low-affinity $\alpha_4\beta_7$. In contrast, the same CC′ loop mutations only slightly decreased cell adhesion mediated by Mn^{2+}-activated $\alpha_4\beta_7$, suggesting the different inter-

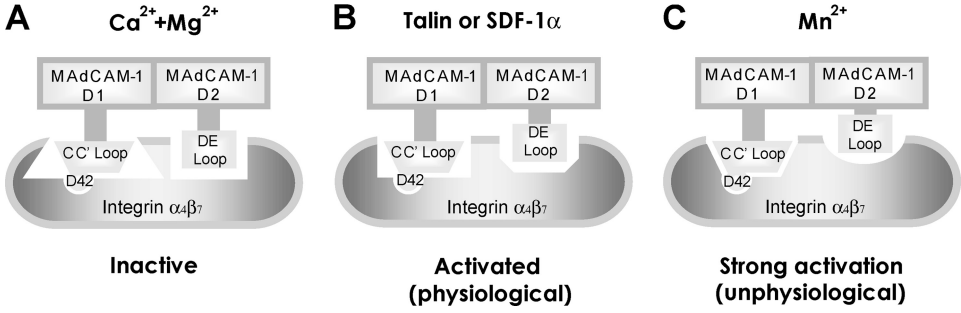

FIGURE 7. **Schematic illustration of distinct interactions between MAdCAM-1 and integrin $\alpha_4\beta_7$ at different activation states.** Integrin $\alpha_4\beta_7$ at different activation states has distinct binding interfaces for the MAdCAM-1 CC′ and DE loops. *A*, binding of MAdCAM-1 to low-affinity (inactive) integrin $\alpha_4\beta_7$. *B*, binding of MAdCAM-1 to high-affinity integrin $\alpha_4\beta_7$ activated by physiological stimuli (talin or SDF-1α). *C*, binding of MAdCAM-1 to high-affinity integrin $\alpha_4\beta_7$ activated by Mn^{2+}.

actions between MAdCAM-1 and Mn^{2+}-activated integrin other than with low-affinity integrin. The reasons that make the CC′ loop subsidiary in supporting $\alpha_4\beta_7$-MAdCAM-1 binding could be due to the stronger interaction between Asp-42 and Mn^{2+} at MIDAS of β_7, and/or there could be additional interactions formed between Mn^{2+}-activated $\alpha_4\beta_7$ and MAdCAM-1.

The DE loop in D2 of MAdCAM-1 is another $\alpha_4\beta_7$ binding interface. Our results showed that the DE loop was less important than the CC′ loop in supporting MAdCAM-1 binding to low-affinity $\alpha_4\beta_7$. Only the removal of the DE loop abolished the interaction between MAdCAM-1 and low-affinity $\alpha_4\beta_7$. Thus, the major function of the DE loop could be to stabilize the interaction between MAdCAM-1 and $\alpha_4\beta_7$, especially the low-affinity integrin. The DE loop is a long and flexible loop exposed on the MAdCAM-1 surface, and its orientation and conformation should be crucial to the MAdCAM-1-$\alpha_4\beta_7$ interaction. Among all of the DE loop single amino acid substitution mutations tested, E152A resulted in the maximal decrease of MAdCAM-1 binding to the low-affinity or talin or SDF-1α-activated $\alpha_4\beta_7$. The MAdCAM-1 crystal structure revealed that the side chain of Glu-152 faces inside the DE loop and protrudes to Glu-158 (9, 10). The Glu-152 side-chain oxygen could form a hydrogen bond with the Asp-158 main-chain oxygen, which might be important to maintain the proper conformation of the DE loop. E152A mutation could lead to loss of this hydrogen bond, which disrupts the optimal conformation of the DE loop for low-affinity $\alpha_4\beta_7$ binding.

Asp-150 is another important residue in the DE loop. E150A mutation decreased the firm cell adhesion mediated by Mn^{2+}-activated $\alpha_4\beta_7$ to the similar level of the DE loop deletion mutant, suggesting its critical position in maintaining the DE loop function. The crystal structure of human MAdCAM-1 showed that Glu-150 could form a hydrogen bond with the Gln-147, which might be important for the control of correct DE loop orientation. E150A mutation could eliminate this hydrogen bond and lead to the rearrangement of DE loop orientation, thus affecting the MAdCAM-1-$\alpha_4\beta_7$ interaction (11).

Another notable finding of our study is the distinct structural requirements for MAdCAM-1 binding to $\alpha_4\beta_7$ activated by Mn^{2+} and more physiological stimuli, such as talin and SDF-1α. In our study, we found that the CC′ loop and the intact DE loop were crucial for MAdCAM-1 binding to integrin $\alpha_4\beta_7$ activated by talin and SDF-1α; however, the MAdCAM-1 binding to $\alpha_4\beta_7$ activated by Mn^{2+} was mostly dependent on Asp-42 and only partially affected by some CC′ and DE loop mutations. Thus, the high-affinity $\alpha_4\beta_7$ activated by Mn^{2+} should have distinct conformation, at least at the ligand-binding interface, than $\alpha_4\beta_7$ activated by talin or SDF-1α through the inside-out signaling.

Acknowledgments—We thank Dr. Minsoo Kim (University of Rochester Medical Center) for kindly providing GFP-talin-head and Dr. Jianping Ding and Dr. Xianchi Dong for discussion.

REFERENCES

1. Springer, T. A. (1994) *Cell* **76,** 301–314
2. Butcher, E. C. (1991) *Cell* **67,** 1033–1036
3. Butcher, E. C., and Picker, L. J. (1996) *Science* **272,** 60–66
4. Gorfu, G., Rivera-Nieves, J., and Ley, K. (2009) *Curr. Mol. Med.* **9,** 836–850
5. Briskin, M. J., McEvoy, L. M., and Butcher, E. C. (1993) *Nature* **363,** 461–464
6. Adams, D. H., and Eksteen, B. (2006) *Nat. Rev. Immunol.* **6,** 244–251
7. Eksteen, B., Liaskou, E., and Adams, D. H. (2008) *Inflamm. Bowel Dis.* **14,** 1298–1312
8. Shyjan, A. M., Bertagnolli, M., Kenney, C. J., and Briskin, M. J. (1996) *J. Immunol.* **156,** 2851–2857
9. Green, N., Rosebrook, J., Cochran, N., Tan, K., Wang, J. H., Springer, T. A., and Briskin, M. J. (1999) *Cell Adhes. Commun.* **7,** 167–181
10. Tan, K., Casasnovas, J. M., Liu, J. H., Briskin, M. J., Springer, T. A., and Wang, J. H. (1998) *Structure* **6,** 793–801
11. Dando, J., Wilkinson, K. W., Ortlepp, S., King, D. J., and Brady, R. L. (2002) *Acta Crystallogr. D Biol. Crystallogr.* **58,** 233–241
12. Viney, J. L., Jones, S., Chiu, H. H., Lagrimas, B., Renz, M. E., Presta, L. G., Jackson, D., Hillan, K. J., Lew, S., and Fong, S. (1996) *J. Immunol.* **157,** 2488–2497
13. Newham, P., Craig, S. E., Seddon, G. N., Schofield, N. R., Rees, A., Edwards, R. M., Jones, E. Y., and Humphries, M. J. (1997) *J. Biol. Chem.* **272,** 19429–19440
14. Chen, J., Salas, A., and Springer, T. A. (2003) *Nat. Struct. Biol.* **10,** 995–1001
15. Briskin, M. J., Rott, L., and Butcher, E. C. (1996) *J. Immunol.* **156,** 719–726
16. Hynes, R. O. (2002) *Cell* **110,** 673–687
17. Luo, B. H., Carman, C. V., and Springer, T. A. (2007) *Annu. Rev. Immunol.* **25,** 619–647
18. Springer, T. A., and Wang, J. H. (2004) *Adv. Protein Chem.* **68,** 29–63
19. Arnaout, M. A., Goodman, S. L., and Xiong, J. P. (2007) *Curr. Opin. Cell Biol.* **19,** 495–507
20. Xiao, T., Takagi, J., Coller, B. S., Wang, J. H., and Springer, T. A. (2004) *Nature* **432,** 59–67
21. Luo, B. H., and Springer, T. A. (2006) *Curr. Opin. Cell Biol.* **18,** 579–586
22. Arnaout, M. A., Mahalingam, B., and Xiong, J. P. (2005) *Annu. Rev. Cell Dev. Biol.* **21,** 381–410
23. Carman, C. V., and Springer, T. A. (2003) *Curr. Opin. Cell Biol.* **15,** 547–556
24. Leitinger, B., McDowall, A., Stanley, P., and Hogg, N. (2000) *Biochim. Biophys. Acta* **1498,** 91–98
25. Chen, J., Takagi, J., Xie, C., Xiao, T., Luo, B. H., and Springer, T. A. (2004) *J. Biol. Chem.* **279,** 55556–55561
26. de Château, M., Chen, S., Salas, A., and Springer, T. A. (2001) *Biochemistry* **40,** 13972–13979
27. Zhu, J., Luo, B. H., Xiao, T., Zhang, C., Nishida, N., and Springer, T. A. (2008) *Mol Cell* **32,** 849–861
28. Xiong, J. P., Mahalingham, B., Alonso, J. L., Borrelli, L. A., Rui, X., Anand, S., Hyman, B. T., Rysiok, T., Müller-Pompalla, D., Goodman, S. L., and Arnaout, M. A. (2009) *J. Cell Biol.* **186,** 589–600
29. Lee, J. O., Rieu, P., Arnaout, M. A., and Liddington, R. (1995) *Cell* **80,** 631–638
30. Chen, J., Yang, W., Kim, M., Carman, C. V., and Springer, T. A. (2006) *Proc. Natl. Acad. Sci. U.S.A.* **103,** 13062–13067
31. Valdramidou, D., Humphries, M. J., and Mould, A. P. (2008) *J. Biol. Chem.* **283,** 32704–32714
32. Pan, Y., Zhang, K., Qi, J., Yue, J., Springer, T. A., and Chen, J. (2010) *Proc. Natl. Acad. Sci. U.S.A.* **107,** 21388–21393
33. Tidswell, M., Pachynski, R., Wu, S. W., Qiu, S. Q., Dunham, E., Cochran, N., Briskin, M. J., Kilshaw, P. J., Lazarovits, A. I., Andrew, D. P., Butcher, E. C., Yednock, T. A., and Erle, D. J. (1997) *J. Immunol.* **159,** 1497–1505
34. Calderwood, D. A., Zent, R., Grant, R., Rees, D. J., Hynes, R. O., and Ginsberg, M. H. (1999) *J. Biol. Chem.* **274,** 28071–28074
35. Kunkel, E. J., and Butcher, E. C. (2002) *Immunity* **16,** 1–4
36. Wright, N., Hidalgo, A., Rodríguez-Frade, J. M., Soriano, S. F., Mellado, M., Parmo-Cabañas, M., Briskin, M. J., and Teixidó, J. (2002) *J. Immunol.* **168,** 5268–5277
37. Erle, D. J., Briskin, M. J., Butcher, E. C., Garcia-Pardo, A., Lazarovits, A. I., and Tidswell, M. (1994) *J. Immunol.* **153,** 517–528
38. Bleul, C. C., Wu, L., Hoxie, J. A., Springer, T. A., and Mackay, C. R. (1997) *Proc. Natl. Acad. Sci. U.S.A.* **94,** 1925–1930